



# Influence of long-chain branching on linear viscoelastic flow properties and dielectric relaxation of polycarbonates

Chenyang Liu<sup>a</sup>, Chaoxu Li<sup>b</sup>, Peng Chen<sup>a</sup>, Jiasong He<sup>a,\*</sup>, Qingrong Fan<sup>b</sup>

<sup>a</sup>State Key Laboratory of Engineering Plastics, Center for Molecular Science, Institute of Chemistry, The Chinese Academy of Sciences, Beijing 100080, China

<sup>b</sup>State Key Laboratory of Polymer Physics and Chemistry, Center for Molecular Science, Institute of Chemistry, The Chinese Academy of Sciences, Beijing 100080, China

Received 26 September 2003; received in revised form 2 January 2004; accepted 17 February 2004

## Abstract

The dynamic viscoelastic property, creep and creep recovery behavior, and dielectric relaxation of long-chain branched Bisphenol A polycarbonates were measured in parallel plate rheometer and dielectric analyzer. The linear polycarbonate (PC-L) as reference and three branched polycarbonates (PC-Bs) have similar molecular weights and molecular weight distributions, while the PC-Bs have different branching degrees, below 0.7 branch points/chain and above twice of  $M_c$ . The long-chain branched polycarbonates exhibit higher zero-shear viscosities, more significant shear thinning, higher flow activation energies, and much longer relaxation times. It was also found that long-chain branches increase the elasticity of melt characterized by the steady-state recoverable compliance and the storage modulus. The 'dissident' rheological behavior of long-chain branching exhibiting mainly in addition polymers such as polyolefin, is confirmed in condensation polymers. These behaviors resulted from additional molecular entanglements of long-chain branches can be understood qualitatively in terms of the tube model for topological constraints. The dielectric  $\alpha$ -relaxation of linear polycarbonate and branched polycarbonates has been fitted with Vogel–Fulcher–Tammann–Hesse (VFTH) equation and the shape of relaxation time curves is also analyzed. The long-chain branched polycarbonates present longer relaxation times, but divergent  $\alpha$ -relaxation temperatures, because the latter is dominated by the free volume.

© 2004 Elsevier Ltd. All rights reserved.

**Keywords:** Long-chain branching in polycarbonate; Rheology; Dielectric relaxation

## 1. Introduction

Polycarbonate (PC) engineering thermoplastics are amorphous, and clear polymers exhibiting three key characteristic properties: toughness, transparency, and heat resistance [1–3]. These qualities, combined with superior dimensional stability and good electrical resistance, have led to wide applications, such as the automobile parts, the electrical parts, the optical materials, and the steam-sterilizable medical equipments. However, PC is not easily processed. Generally, making PC more processable, decreases the toughness and impairs its value for engineering applications.

Branching and alloying are two techniques commonly

used to achieve a high-flow PC resin while maintaining other properties. A number of investigations have been conducted on blend systems of polycarbonate and other polymers, including ABS and SAN [4–6], polyolefins [7,8], polyesters [9,10], and others [11–13]. However, branching PC is the only way to keep the transparency, and suppliers of PC resins have developed and provided high-flow clear resins [14–16] to meet these demands. Branching of polycondensates is usually achieved by incorporation of a branching agent. After giving the statistical distribution of the branched segments in polymers, such polymers are called randomly branched and divided into short-chain branched and long-chain branched according to its structure. Those polymers with a weight-average molecular weight per arm ( $M_w/arm$ ) greater than the critical molecular weight for entanglements,  $M_c$  [17], can be called long-chain randomly branched, contrarily be called short-chain randomly branched. The commercial long-chain branched

\* Corresponding author. Tel.: +86-10-6261-3251; fax: +86-10-6255-9373.

E-mail address: [hejs@sklep.icas.ac.cn](mailto:hejs@sklep.icas.ac.cn) (J. He).

polycarbonates are manufactured for their greater degrees of melt strength and shear-rate sensitivity [15,16,18,19].

All the while, the influence of long-chain branching (LCB) in polymers on the rheological properties has attracted considerable interest both in the research community and in industry [17,20,21]. Recently, with the advent of metallocene and other ‘single-site’ catalysts, the polyethylene rheology is focused on the effect of LCB on the linear viscoelastic behavior of polyethylenes and the determination of the LCB level in metallocene polyethylenes by using rheological data [22–26]. Metallocene polyethylene, such as HDPE or LLDPE, which possesses low amounts of LCB, displays rheological features in dynamic viscosity, relaxation time, elastic modulus, activation energy of flow, and melt strength. This principle has been applied mainly to addition polymers such as polyolefin, which is rarely confirmed in condensation polymers. The branched aliphatic polyesters [27,28] prepared by introducing a branching agent into the polycondensation system also exhibited ‘dissident’ rheological behaviors. However, there is no report on the rheology of the commercially branched polycarbonates, except that mechanical and rheological behaviors of linear and branched PC blends have been studied [14]. So, it is worthwhile to explore the influence of long-chain branches in polycondensate on linear viscoelastic flow properties in theory and applications.

In the present work, because a linear and three branched polycarbonates have similar molecular weights and molecular weight distributions (MWDs), this offers the possibility of studying the influence of LCB on linear viscoelastic flow properties and dielectric relaxation without the need to take into account the influence of polydispersity. The dynamic viscoelastic properties, creep and creep recovery measurements, and dielectric relaxations were investigated for the three branched Bisphenol A polycarbonates and the linear one. Based on these results, discussion is made on of the influence of long-chain branches incorporated in polycarbonates on the rheological properties such as zero-shear viscosity, the shear thinning, the elastic modulus and loss angle, the flow activation energy  $E_a$ , and the steady-state recoverable compliance  $J_e^0$ . The influence of long-chain branches on  $\alpha$ -relaxation and relaxation time curve is also discussed.

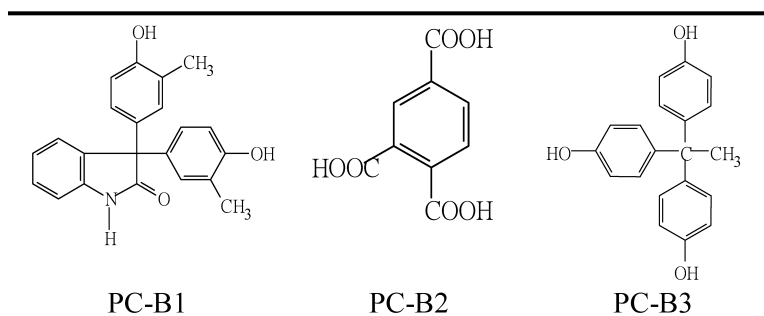
## 2. Experimental

### 2.1. Materials and characterization

Three branched Bisphenol A polycarbonates (PC-B1–B3) investigated were supplied as pellets by Bayer, General Electric Plastic, and Idemitsu Petrochemical Co., respectively. A linear polycarbonate (PC-L) was used as a reference, supplied by Idemitsu Petrochemical Co. All these samples were used as received. The molecular parameters of materials, such as  $M_w$  and  $M_w/M_n$ , were measured on a Waters 510 GPC instrument. The temperature for the measurements was 40 °C, and the solvent used was THF. The chemical structure of three different branching agents for PC-Bs is shown in Scheme 1. The incorporation content of branching agents was determined by using base-hydrolysis, followed by high performance liquid chromatography (HPLC) [29,30]. For PC-B1, this result was verified further by  $^1\text{H}$  NMR measurement. Quantified as the weight-average molecular weight per arm ( $M_w/\text{arm}$ ), the term ‘long-chain branched’ can be used to describe polymers with  $M_w/\text{arm}$  greater than the critical molecular weight for entanglement,  $M_c$ . Here PC-B1, a representative of branched PC-Bs, has about 0.7 branch points/chain, which equals to the repeat units per molecule multiplied by the molar content of branching agents ( $34,700/254 \times 0.5\%$ ). Therefore, the average  $M_w/\text{arm}$  of PC-B1 should be beyond 10,000 g/mol and greater than  $M_c$  which is about 4000 g/mol [31] or 4800 g/mol [32], then PC-B1 is a star polymer possessing an amount of long-chain branches whose value should not be more than the content of branching agents. The glass transition temperatures ( $T_g$ ) of PCs, were determined by means of a Perkin–Elmer DSC-7. All the molecular and physical parameters are listed in Table 1.

### 2.2. Rheological measurements

Dynamic and steady shear rheological measurements were carried out on a Rheometrics SR 200 dynamic stress rheometer. The samples were melt pressed at 260 °C into 1 mm thick plates, and then were cut into small disks about 25 mm diameter. Before rheological measurements,



Scheme 1. Chemical structures of three different branching agents for PC-Bs.

Table 1  
Characteristics of the polycarbonates studied

Samples	Suppliers and codes	$M_w$ (g/mol)	$M_w/M_n$	Branching agents	Degree of branching <sup>a</sup> (mol%)	$T_g$ (°C)
PC-L	Idemitsu A 2700	35,500	3.03	–	–	154.5
PC-B1	Bayer M-3118	34,100	3.72	3,3-Bis(3-methyl-4-hydroxyphenyl)oxyindole	0.5 (0.4 <sub>3</sub> ) <sup>b</sup>	150.2
PC-B2	GE Lexan 154	34,700	3.79	Trimellitic acid	0.5	151.0
PC-B3	Idemitsu IB 2500	37,100	3.52	1,1,1-Tris(4-hydroxyphenyl)ethane	0.3	153.5

<sup>a</sup> Estimated by using hydrolysis-HPLC methods.

<sup>b</sup> Estimated by using <sup>1</sup>H NMR.

samples were annealed in a vacuum oven at 155 °C for 1 h to completely remove the moisture. These measurements were then run with 25 mm parallel plate geometry and a 1 mm sample gap. Thermal stability of samples during the rheological testing was checked by a time sweep, where the selected samples gave a stable  $G'$  signal for at least 100 min at 260 °C. The dynamic viscoelastic properties were determined with frequencies from 0.1 to 500 rad/s, by using strain values determined with a stress sweep to lie within the linear viscoelastic region (LVR). The steady-state shear experiment followed the oscillatory shear experiment on the same sample. All measurements were carried out in nitrogen atmosphere at three different temperatures 240, 260 and 280 °C.

The shear creep and creep recovery measurements were conducted by using stress-controlled air bearing shear rheometer (Rheometrics SR-200). Samples were measured at temperature of 220 °C in a parallel plate geometry with a diameter of 25 mm and a gap of 1 mm. Creep experiments followed by recovery were carried out at different stress levels (from 10 to 100 Pa), in order to assure the linearity of the experimental response. Shear stresses of about 50 Pa are well within the range of linear viscoelastic behavior for these materials. To avoid the interference of a small residual torque of the bearing of the rheometer superimposed in the recovery experiment, the recovery data presented in this article were corrected, according to the drift correction described in paper of Gabriel and Kaschta [33].

### 2.3. Dielectric relaxation spectroscopy

Dielectric measurements were performed by using the dielectric analyzer, DEA 2970 (TA Instruments). Films with the thickness of ca. 0.3–0.4 mm were sandwiched between the ceramic parallel plate sensors (the diameter was 25 mm), and exerted by a maximum force of ca. 100 N to insure good contact between the sample and the electrodes. The experiments were performed within a temperature range from 20 to 190 °C at the heating rate of 1 °C/min, and a frequency range from 1 to 10<sup>5</sup> Hz. And also frequency scans were performed at constant temperature, which was increased in steps (the temperature stability was better than 0.2 K). The DEA cell was purged with dry nitrogen adjusted to a flow rate of ca. 500 ml/min.

## 3. Results and discussion

### 3.1. Viscoelastic properties

#### 3.1.1. Shear rate dependence of viscosity

Typically the viscosity of molten polymers approaches a constant value  $\eta_0$  at lower shear rates, and begins to deviate from  $\eta_0$  at some characteristic shear rate. At higher shear rates the viscosity approaches ‘power law’ behavior. Dynamic viscosity curves for linear and branched polycarbonates at 260 °C are shown in Fig. 1, together with the steady viscosity obtained from steady stress sweep experiments. For each sample, one can observe that the low shear rate viscosity plateau broadly spans to 10<sup>-2</sup> s<sup>-1</sup> and that the Cox–Merz rule [34] is quite well verified. Both observations allow the determination of the zero-shear viscosity  $\eta_0$  with satisfactory accuracy. The values of  $\eta_0$  are listed in Table 2. PC-L has the lowest zero-shear viscosity, though PC-B1 and PC-B2 have a little low molecular weight. It can be seen from Fig. 1 that at low shear rate the viscosities of all branched PC-Bs are much higher than that of PC-L. However, at high frequency the viscosities of all PC-Bs are lower than that of PC-L, and the viscosities of the formers begin to decrease with shear rate much sooner than that of the latter. The onset of frequency dependence of viscosity (non-Newtonian, shear-thinning behavior) can be defined as a characteristic frequency  $\omega_0$ , at which  $\eta(\omega_0) = 0.8\eta_0$  according to the Graessley’s empirical formula [35]. The

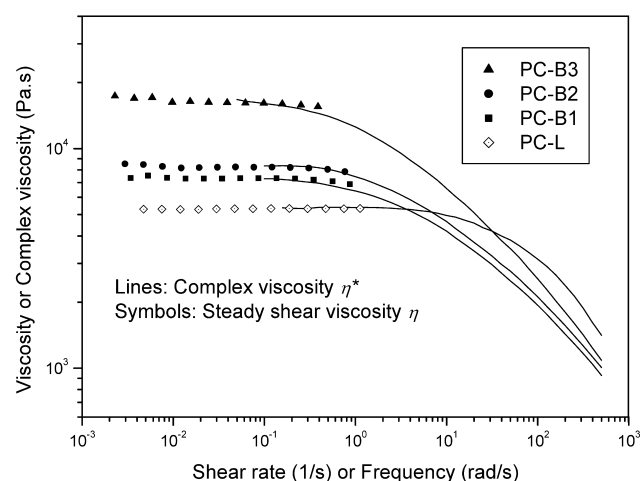


Fig. 1. Viscosity vs. rate for linear PC-L and branched PC-Bs at 260 °C.

Table 2  
Rheological data of the linear and branched polycarbonates

Samples	$\eta_0$ 260 °C (Pa s)	$\omega_0$ (rad/s)	$\lambda_0$ (s)	$G' - G''$ slope	$E_a$ (kJ/mol)	$J_e^0$ (recovery) ( $\times 10^{-6}$ Pa $^{-1}$ )	$J_e^0$ (dynamic) ( $\times 10^{-6}$ Pa $^{-1}$ )
PC-L	5400	26.8	0.022	2.0 <sub>3</sub>	109 $\pm$ 3	–	5
PC-B1	7720	1.3	0.46	1.6 <sub>4</sub>	117 $\pm$ 4	68	90
PC-B2	8850	0.93	0.65	1.6 <sub>4</sub>	121 $\pm$ 2	66	81
PC-B3	17,800	0.45	1.33	1.6 <sub>0</sub>	121 $\pm$ 2	85	119

values of  $\omega_0$  are also listed in Table 2. The characteristic frequencies of three branched PC-Bs are 1–2 decades lower than that of PC-L, indicating that the branched PC-Bs exhibit higher shear sensitivities.

The extent of shear thinning and the onset shear rate for shear thinning are related with two factors: chain branching, and MWD [17,36]. The linear and branched polycarbonates have similar molecular weights and MWDs. However, the branched PC-Bs exhibit higher zero-shear viscosities and more significant shear thinning, which is consistent with the rheological behavior of polyethylenes and polyesters possessing an amount of long-chain branches [22–24,27,28].

There are two effects of the LCBs on the viscosity curves of polymers. On one hand, LCBs are more helpful to molecular entanglement than the linear polymer of the same molecular weight, if they have the same chemical structure. At low shear rates, polymers with long chain branches would have higher viscosity than linear polymers. On the other hand, the branched polymer is easier to be disentangled under shear than the linear polymer [17,36]. Thus, shear thinning becomes more noticeable with increasing long chain branch density. The notable shear thinning of the branched PC-Bs indicates that the modified polycarbonates prepared by incorporating 0.3–0.5 mol% branching agents have chain branches long enough to produce molecular entanglements. Consequently, the commercial branched PC-Bs will exhibit high melt strengths, high shear

sensitivities, which will provide better processabilities particularly in blow molding applications.

### 3.1.2. Storage modulus and loss modulus

Fig. 2 shows a comparison of storage and loss modulus for PC-L and PC-B1 at 260 °C. As expected, at the temperature and frequency the rheological measurements were carried out, the molecular chains of the linear PC-L are fully relaxed and exhibit characteristic behavior in the terminal zone, where  $G'$  is proportional to  $\omega^2$  and  $G''$  is proportional to  $\omega$ . However, PC-B1 has a higher value of storage (elastic) modulus in terminal zone, and a similar frequency dependence of loss modulus. Elastic properties enhanced with LCBs can also be observed in Fig. 3. Three branched PC-Bs have higher modulus than the linear PC-L in terminal zone. Chain branching adds a mode of relaxation at low frequency that is not present in the linear polymer. This behavior can be understood qualitatively in terms of the tube model for topological constraints [17,36,37]. The increase in the storage modulus was a sensitive indicator of LCBs for branched polybutadienes [38], polyethylenes [22–24], and polyesters [27,28].

It should be noted from Figs. 2 and 3 that the branched PC-Bs have lower modulus than the linear PC-L at high frequencies. The similar phenomena were reported for branched polymers in the polybutadiene and polyisoprene star-linear blending systems [39], respectively. It needs

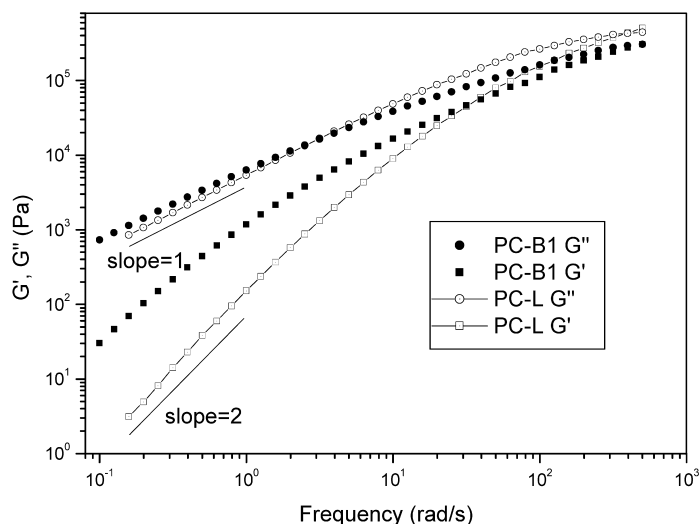


Fig. 2. The comparison of storage and loss modulus for PC-L and PC-B1 at 260 °C.

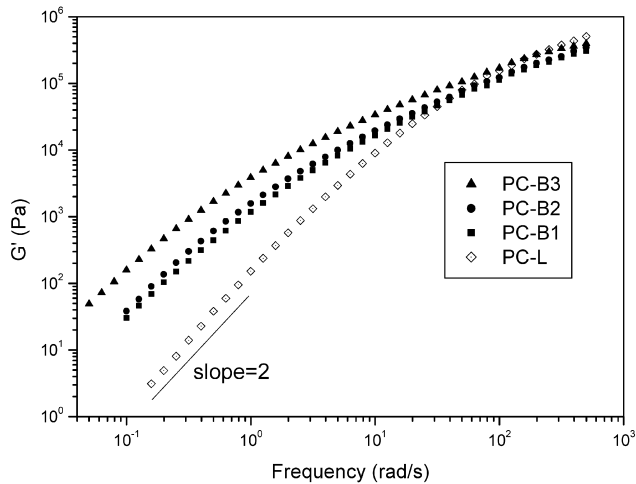


Fig. 3. Effect of LCBs on the storage modulus ( $G'$ ) for linear PC-L and branched PC-Bs at 260 °C.

more experimental and theoretical work to explain this peculiar phenomenon.

The plots of storage modulus ( $G'$ ) vs. loss modulus ( $G''$ ) have been used by Han et al. [40–42] to investigate the changes in the microstructure of polymers or blends. In general, most isotropic homogeneous polymer melts and solutions give a slope of 2 on the logarithmic plot of  $G'$  against  $G''$ , whereas heterogeneous polymeric systems such as mesophase and block copolymers show the slopes lower than 2 [41,42]. Kim et al. [27,28] used  $\log G'$  vs.  $\log G''$  to explore the influences of branching of aliphatic polyesters on the microstructures. Fig. 4 shows the plots of  $G'$  vs.  $G''$  for linear PC-L and branched PC-Bs at 260 °C, and the terminal slopes are listed in Table 2. The terminal zone slope of linear PC-L is 2, but the slope decreases to the vicinity of 1.6 with introducing LCB to the PC-Bs. This suggests that long chain branches make the melt a little more heterogeneous, which is consistent with loss angle behavior to be discussed below.

Loss angle vs. frequency for linear PC-L and branched

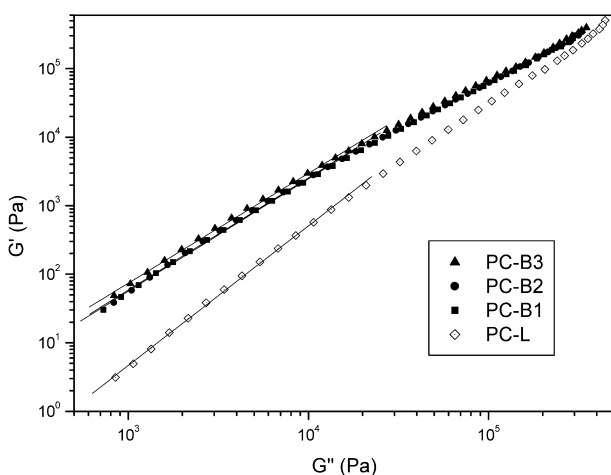


Fig. 4. Plots of storage modulus ( $G'$ ) vs. loss modulus ( $G''$ ) for linear PC-L and branched PC-Bs at 260 °C. The solid lines represent the terminal slopes.

PC-Bs are shown in Fig. 5. The loss angle curve for the linear PC-L shows a typical behavior for linear polymers: the angle increases quickly and approaches the value of 90° in the terminal flow region, meaning the sample is highly viscous. The behaviors of the branched PC-Bs are quite different from that of the linear polymer. Wood-Adams et al. [24] reported that there was a plateau in the loss angle, the magnitude and breadth of which depended on the degree of LCB in polyethylenes. Here, the plateaus in the loss angle are not observed for the PC-Bs, but the loss angles of the PC-Bs are lower and do not arrive the value of 90° even at the lowest frequency where the rheological measurements were carried out. This observation is in accordance with the results of Kim et al. [27,28], who noted the same effect of LCB on loss factor when comparing the linear and branched polyesters, and believed that polyesters with LCB exhibited more notable elastic properties or solid characters.

### 3.1.3. The flow activation energy

The temperature dependence of the viscosity of polymer melts is one of the most important parameters in polymer flow. For the temperature range of about 100 °C above the  $T_g$ , the temperature dependence of the viscosity of polymer melts can be expressed in the Arrhenius form:

$$\eta_0 = A \exp(E_a/RT) \quad (1)$$

where  $\eta_0$  is the zero shear viscosity,  $R$ , the gas constant,  $A$ , a constant,  $E_a$  is called the flow activation energy.  $E_a$  varies widely from polymer to polymer, and depends on chain composition. The higher the  $E_a$ , the more temperature sensitive is the melt. However,  $E_a$  is independent of polymer molecular weight and distribution, so long as the molecular weight exceeds a minimum value corresponding closely to the entanglement molecular weight [43].

Fig. 6 shows the Arrhenius plots for linear PC-L and branched PC-Bs. Values of  $E_a$  are calculated by using  $\eta_0$  data at temperatures from 240 to 280 °C and are listed in

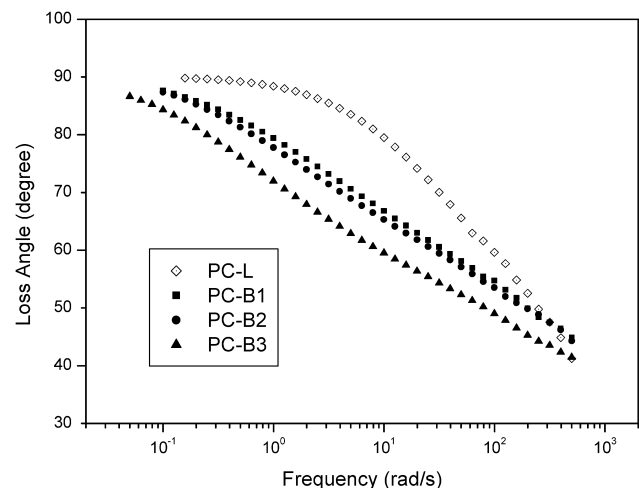


Fig. 5. Loss angle vs. frequency for linear PC-L and branched PC-Bs at 260 °C.



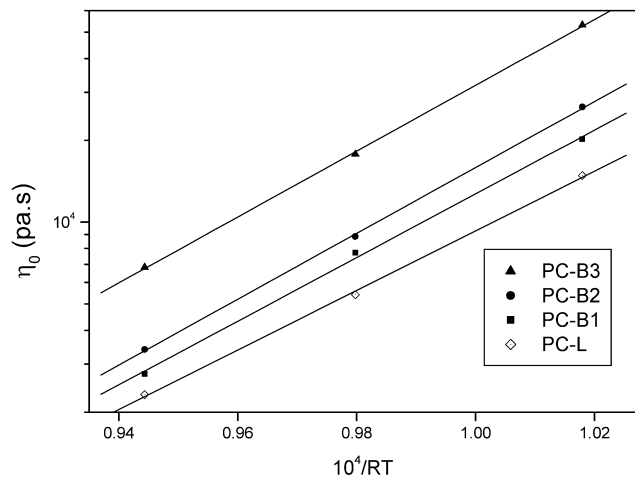


Fig. 6. Arrhenius plots for linear PC-L and branched PC-Bs.

**Table 2.** It is clear that the  $E_a$  increases with the introduction of LCB to the PC-Bs, that is 109 kJ/mol for PC-L to about 120 kJ/mol for PC-Bs. The flow activation energy of PC-L is in good agreement with the value of 26 kcal/mol (109 kJ/mol) reported by Wang and Porter [43]. The increase in the flow activation energy due to the presence of long-chain branches is a well-known phenomenon for statistically branched polymers. This phenomenon is also observed for star-like polymers [44] and polyethylenes with low amounts of LCB by Vega et al. [22]. The latter also recommended the calculation of a ‘LCB index associated to activation energy of flow’ by subtracting the activation energy of flow of a linear polymer from that of polymer with LCB. Because the flow activation energy is not influenced by  $M_w$  and MWD, the relatively high flow activation energy of PC-Bs are therefore a strong argument that the PC-Bs actually contain long-chain branches.

### 3.2. Elastic properties: the creep and creep recovery

The steady-state recoverable compliance  $J_e^0$  of a polymer melt is a useful property for a measure of its elasticity. At low molecular weight  $J_e^0$  is proportional to the molecular weight, but above a critical molecular weight  $M_c'$  it becomes constant [17]. In addition, the recoverable compliance  $J_e^0$  is extraordinarily sensitive to MWD and LCB [17,36]. Because the linear and branched polycarbonates have similar molecular weights and MWDs, this offers the possibility of studying the influence of LCB on the elastic properties of polycarbonate melts without the need to take into account the influence of polydispersity.

With regard to the principle of the creep and creep recovery experiments, Gabriel and Kaschta [33] have a detailed description with its main points as follows. The time-dependent creep compliance in the linear viscoelastic regime can be calculated as

$$J(t) = \frac{\gamma(t)}{\tau_0} \quad (2)$$

and the recoverable compliance  $J_r(t, t_0)$  follows from the recoverable part of the shear deformation  $\gamma_r(t, t_0)$  as

$$J_r(t, t_0) = \frac{\gamma_r(t, t_0)}{\tau_0} \quad (3)$$

Only in the case that a constant shear rate is reached in the preceding creep test, the recoverable compliance is independent of the creep time  $t_0$ . After a very long creep time  $t_0$  and recovery time  $t$  the recoverable deformation reaches a constant value  $\gamma_e^0$ , and the steady-state recoverable compliance in the linear range of deformation  $J_e^0$  can be calculated as

$$J_e^0 = \frac{\gamma_e^0}{\tau_0} \quad (4)$$

In both experiments the time scale is critical, as one has to be sure that the steady state has been reached. The creep and recoverable compliances as a function of time are shown in Fig. 7 for linear PC-L and branched PC-Bs at 220 °C. The dashed lines of a slope 1 indicate the creep equilibrium approached, and it verifies the validity of the steady-state recoverable compliance  $J_e^0$  of all PCs. However, the recoverable compliance  $J_e^0$  for PC-L cannot be acquired in the recovery experiment due to the very small elasticity of the melt. Fortunately, an alternative way of determining  $J_e^0$  is from dynamic modulus at the zero-frequency limit [17]:

$$J_e^0 = \frac{\psi_{1,0}}{2\eta_0^2} = \lim_{\omega \rightarrow 0} \left( \frac{G'}{(G'')^2} \right) \quad (5)$$

where  $\psi_{1,0}$  is the first normal stress coefficient. This method of determination only requires the limiting slopes of 1 and 2 for  $G''$  and  $G'$  on a double-logarithmic plot to be achieved.

The results from both recovery and dynamic experiments are summarized in Table 2. The values from the recovery experiments are consistently lower than those from the dynamic experiments. The phenomenon was also reported in the literature [31]. As can be seen from Table 2,  $J_e^0$

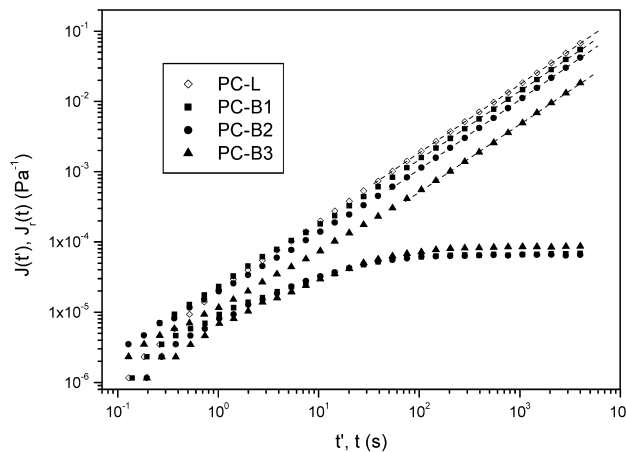


Fig. 7. Creep and recoverable compliances as a function of time for linear PC-L and branched PC-Bs at 220 °C. The dashed lines of a slope 1 indicate the creep equilibrium.

increases by more than 1 decade with incorporating a low amount of LCB. The recoverable compliance  $J_e^0$  of linear PC-L is accordant with the value of  $5$  or  $6 \times 10^{-6} \text{ Pa}^{-1}$  reported in the literature [31]. Because the branched PC-Bs have similar molecular weights and MWDs with the linear PC-L, long chain branches are responsible for the increase in the elasticity of polymer melts. It has been observed that  $J_e^0$  of LCB polymer is larger than linear polymer, and often enormously so, as much as a factor of 10 for star polymers [45–47]. The results for the linear and branched PCs with similar MWD are further evidence for the LCB on the elastic properties of polymer melts in the linear regime. Finally, the higher elasticity is also consistent with the higher frequency-dependent storage modulus in terminal zone for PC-Bs discussed in Section 3.1.2 (Fig. 3).

Wimberger-Friedl et al. [31] investigated the effect of chain stiffness of copolycarbonates containing a spiro-linkage on the rheological and mechanical properties of these materials. When the content of stiff spiro monomer (SBI) is beyond 50% in mol percentage, the recoverable compliance  $J_e^0$  increases by about 1 decade compared with the Bisphenol A homopolymer. In our investigation, the incorporation of 0.3–0.5 mol% LCB increases the  $J_e^0$  up to a higher level than the incorporation of 65% stiff spiro monomer. Therefore, it is concluded that for improving the elasticity of polycarbonate, to introduce the LCB is more effective than to introduce the stiff units into the main-chain.

The viscoelastic properties in the terminal zone are dominated by characteristic constants [17]  $\eta_0$ ,  $J_e^0$ ,  $\psi_{1,0}$ , and the terminal relaxation time  $\lambda_0$  which was obtained from the characteristic frequency  $\omega_0$  [35]:

$$\omega_0 \lambda_0 = 0.6 \quad (6)$$

Here, the entanglements have their maximum effect in influencing the properties, which reflect the longest-range molecular motions. Graessley [48] or Doi–Edwards theories [49] interrelate the effects of different variables on these three terminal zone constants:

$$\lambda_0 = \eta_0 J_e^0 \quad (7)$$

In Fig. 8 the experimental  $J_e^0$  is plotted vs.  $\lambda_0/\eta_0$  for all polycarbonates (solid symbols from creep recovery; open symbols from dynamic modulus), and diagonal line represents Eq. (7). It is obvious that the experimental values of  $J_e^0$  for PCs agree reasonably with Eq. (7). The Graessley equation is originally employed in the correlation of terminal zone constants of the linear polymers with narrow MWD. It is surprising that Eq. (7), and presumably also Eq. (6), holds also for the PC-Bs with a low amount of LCB, although the recoverable compliance  $J_e^0$  increases by more than 1 decade. Since both  $\eta_0$  and  $J_e^0$  are enhanced by LCB, it follows that the terminal relaxation time  $\lambda_0$  is greatly increased, corresponding to the decrease in  $\omega_0$  (Table 2) which is apparent in the onset of non-Newtonian viscosity [17]. Gabriel and Munstedt [47] noted the similar difference of creep and recovery properties between two mLLDPEs

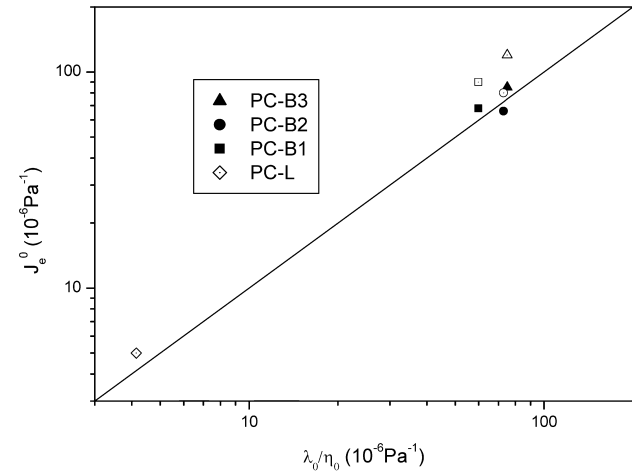


Fig. 8. Steady-state recoverable compliances vs.  $\lambda_0/\eta_0$ : solid symbols from creep recovery; open symbols from dynamic modulus. Diagonal line represents the Graessley equation:  $\lambda_0 \cong \eta_0 J_e^0$ .

(one contained long-chain branches). LCB also affects the low-frequency side of the dielectric relaxation time, which will be discussed below. By comparing creep recovery measurements of linear and branched PCs, the conclusion could be drawn that LCB is responsible for the higher melt elasticity and the longer relaxation times of the PC-Bs.

### 3.3. Influence of long-chain branching on the dielectric relaxation

It is well known that the primary relaxation is produced by the micro-Brownian motion of the polymer chain segments and is associated with the glass transition. The dielectric  $\alpha$ -relaxation of polymers, generally appearing at temperatures around and above  $T_g$  of DSC measurement, was always characterized by a distribution of relaxation times, reflecting in some manner the local molecular structure [50,51]. Typically, if the dielectric experiment is performed within a frequency range from 10 to  $10^5$  Hz, the  $\alpha$ -peak will correspond to  $T_g(\text{DSC}) + 10\text{--}20$  K [52].

Fig. 9 shows the Arrhenius plots of the peak frequencies for the dielectric  $\alpha$ -relaxation of linear PC-L and branched PC-Bs. It is found that at the same peak frequency, PC-B1 and PC-B2 have lower  $T_g$ s, but PC-B3 has a little higher  $T_g$ , compared with linear PC-L. This order is qualitatively consistent with the DSC measurement, and the LCB does not always increase  $T_g$ . The result reflects that the factors influencing the  $\alpha$ -relaxation temperature, i.e. motion ability of chain segments, are complicated. Wang and Porter [43] illustrated the effects of chain branching on  $T_g$ . On one hand, the substitution of a branch for a linear molecule can increase free volume and decrease  $T_g$ , which is analogous that the end-groups in lower molecular weight polymers increase free volume and decrease  $T_g$  [53]. On the other hand, for long chain branches, adding molecular entanglements, which will restrict the segmental motions of the polymer, may induce a retarded  $\alpha$ -relaxation [50] and raise

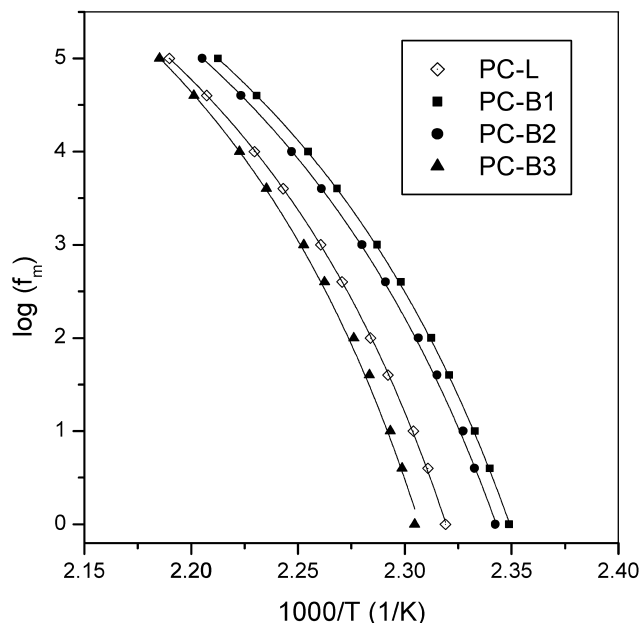


Fig. 9. Dielectric loss curve peak frequency ( $\log f_{\max}$ ) as a function of reciprocal temperature for the dielectric  $\alpha$ -relaxation of linear PC-L and branched PC-Bs. The solid lines represent the fitting results with the VFTH equation.

$T_g$ . Here, the first effect is prevailing, because PC-B1 and PC-B2 have higher branching degree of 0.5 mol% than PC-B3 of 0.3 mol%, so that lower  $T_g$ s. Oppositely, PC-B3 with lower branching degree should have presumable longer branching chain, then have almost identical  $T_g$  with PC-L at both DSC and dielectric measurements.

Based on free-volume theory, this type of  $\alpha$ -relaxation behavior can be described by the empirical VFTH equation [54]:

$$f_{\max} = A \exp[-B/(T - T_0)] \quad (8)$$

where  $T_0$  is called Vogel temperature or the ideal glass transition temperature, and is typically 30–60 K below  $T_g$ . The solid lines in Fig. 9 represent the fitting results of the  $\alpha$ -relaxation data of PCs with the VFTH equation. As can be seen, a good overall fit is obtained for all polycarbonates, and the fitting results are presented in Table 3. These Vogel temperatures,  $T_0$ s, are comparable with the value of 385 K reported in the literature for PC [55]. Zhong et al. [56] suggested that the temperature dependence of activation energy for  $\alpha$ -relaxation process could be expressed in terms

Table 3  
Fitting parameters of the VFTH analysis

Samples	$\log A$	$B$	$T_0$ (K)
PC-L	10.5	683	403.0
PC-B1	10.7	735	395.8
PC-B2	10.8	766	396.0
PC-B3	10.8	696	405.5

of parameters  $B$  and  $T_0$  in the VFTH equation:

$$E_a = \frac{RB}{(1 - T_0/T)^2} \quad (9)$$

Fig. 10 shows the activation energy vs. temperature according to Eq. (9). Obviously, for each sample its activation energy increases with decreasing temperature, and increases rapidly as the temperature approaches  $T_g$ . The temperature dependence of activation energy is a characteristic of  $\alpha$ -relaxation process based on the free volume concepts [36,43]. Therefore, it could be understood that the values from 480 to 835 kJ/mol have been reported in the literature for PC [57]. In the whole temperature range studied, PC-B1 and PC-B2 have lower  $E_a$ , and PC-B3 has a higher value, than linear PC-L, which is consistent with above results in Fig. 9.

A line shape analysis of the  $\alpha$ -relaxation spectra provides an insight into the molecular mechanism of the relaxation for linear PC-L and branched PC-Bs. The dielectric  $\alpha$ -relaxations of polycarbonates at 167 °C are plotted in Fig. 11, after the normalization for a comparison of their peak widths. First, the skewed distribution at higher frequencies (high frequency broadening) is characteristic of many polymer systems and has been addressed theoretically by Davidson and Cole [58]. It can also be found that the branched PC-Bs have wider relaxation peaks than the linear PC-L, showing broader relaxation time distributions or less homogeneous relaxing environment. And also there is an apparent deviation in the low-frequency side but less in the high-frequency side, according to dielectric theory [59], which means a larger percentage of relaxing dipoles with longer relaxation times. It further confirms the effects of LCBs on the molecular entanglements, and the terminal relaxation time  $\lambda_0$  is greatly increased (Section 3.2).

The influence of LCB in polycarbonates on dielectric  $\alpha$ -relaxation is more complicated than on the linear viscoelastic flow properties. The rheological behaviors of

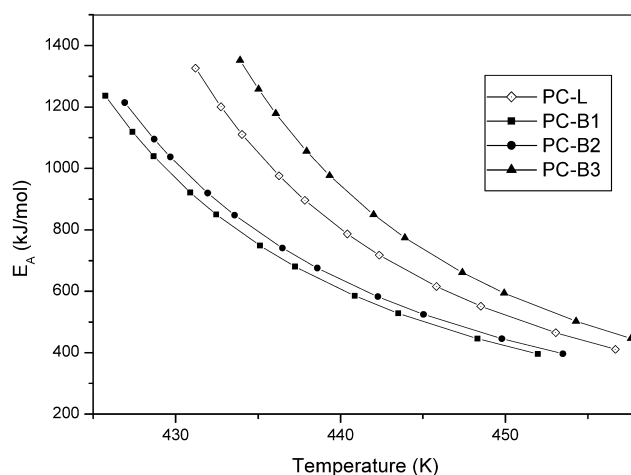


Fig. 10. Activation energy from a general formula Eq. (9) composed of VFTH parameters for linear PC-L and branched PC-Bs.



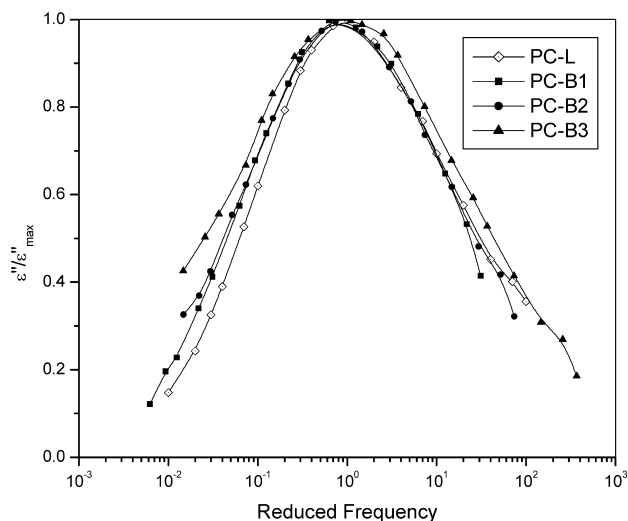


Fig. 11. Normalized spectra of dielectric loss factor  $\epsilon''$  against frequency  $f$  at 167 °C, where  $f_{\max}$  is the frequency at which there is a maximum in dielectric loss factor  $\epsilon''_{\max}$ .

LCB can be understood qualitatively by considering additional molecular entanglements, whereas the dynamics of molecular motions at the liquid–glass transition are mainly involved in the free volume. The free volume can be studied by positron annihilation lifetime spectroscopy (PALS), and the motion ability of chain segments may be studied by enthalpy relaxation through physical aging processes, which will be investigated in depth in future work.

#### 4. Conclusions

The influence of LCB in polycarbonates on linear viscoelastic flow properties and dielectric relaxation has been investigated. The linear polycarbonate (PC-L) and branched polycarbonates (PC-Bs) with different branching agents and contents have similar molecular weights and MWDs, therefore the effect of polydispersity on rheological properties does not need to be taken into consideration. The long-chain branched polycarbonates exhibit higher zero-shear viscosities, more significant shear thinning, higher flow activation energies, and much longer relaxation times. It is also found that long-chain branches increase the elasticity of melt, characterized by the steady-state recoverable compliance and the storage modulus. These findings are consistent with the results of polyethylenes and aliphatic polyesters possessing an amount of long-chain branches in the literatures. These behaviors resulted from adding molecular entanglements of long-chain branches can be understood qualitatively in terms of the tube model for topological constraints.

The dielectric  $\alpha$ -relaxations of linear polycarbonate and branched polycarbonates have been fitted with a Vogel–Fulcher–Tammann–Hesse (VFTH) equation and the

temperature dependence of activation energy for  $\alpha$ -relaxation is discussed. The divergent  $\alpha$ -relaxation temperatures of PB-Bs are due to the influence of branching on the free volume. The branched PC-Bs have wider relaxation peaks than the linear PC-L, showing broader relaxation time distributions or less homogeneous relaxing environment. Especially the apparent deviations in the low-frequency side show longer relaxation times.

It can be concluded that polycarbonates incorporating with LCB show above dissident rheological behaviors, which were observed previously in addition polymers such as polyolefin. The influence of LCB in polycarbonates on dielectric  $\alpha$ -relaxation can be explained by the free volume concept, besides the molecular entanglements. Finally, the results manifest that the commercial branched PC-Bs will exhibit high melt strengths, high shear sensitivities, which will provide better processabilities particularly in blow molding applications.

#### Acknowledgements

This work is supported by National Natural Science Foundation of China (Grant No. 50233010). The authors acknowledge the IUPAC project (No. 421/35/97) for the collection of samples. The authors are also grateful to Professors T. Masuda, M. Takahashi and T. Takigawa for their coordination of this IUPAC project.

#### References

- [1] Pham HT, Munjal S, Bosnyak CP. Polycarbonates. In: Olabisi O, editor. Handbook of thermoplastics. New York: Marcel Dekker; 1997.
- [2] Madkour TM. Polycarbonate. In: Mark JE, editor. Polymer data handbook. New York: Oxford University Press; 1999.
- [3] Pham HT, Weckle CL, Ceraso JM. *Adv Mater* 2000;12:1881–5.
- [4] Greco R, Astarita MF, Dong L, Sorrentino A. *Adv Polym Technol* 1994;13:259–74.
- [5] Greco R, Sorrentino A. *Adv Polym Technol* 1994;13:249–58.
- [6] Kim WN, Burns CM. *J Appl Polym Sci* 1990;41:1575–93.
- [7] Huang JC, Shen HF, Chu YT. *Adv Polym Technol* 1994;13:49–55.
- [8] Mascia L, Valenza A. *Adv Polym Technol* 1995;14:327–35.
- [9] Factor BJ, Mopsik FI, Han CC. *Macromolecules* 1996;29:2318–20.
- [10] Hashemi S. *Polym Engng Sci* 1997;37:912–21.
- [11] Kim WN, Park CE, Burns CM. *J Appl Polym Sci* 1993;49:1003–11.
- [12] Ohishi H, Ikehara T, Nishi T. *J Appl Polym Sci* 2001;82:2566–82.
- [13] Zhang MZ, Choi P, Sundararaj U. *Polymer* 2003;44:1979–86.
- [14] Lyu MY, Lee JS, Pae Y. *J Appl Polym Sci* 2001;80:1814–24.
- [15] Scott SW. US Patent 4,001,184; 1977.
- [16] Idel KJ, Freitag D, Nouvertne W. US Patent 4,185,009; 1980.
- [17] Ferry JD. *Viscoelastic properties of polymers*, 3rd ed. New York: Wiley; 1980. Chapters 10 and 13.
- [18] Kuze S, Okumura R, Takahashi S. US Patent 5,473,046; 1995.
- [19] Day J, Hait SB. US Patent 6,365,703; 2002.
- [20] Graessley WW. *Acc Chem Res* 1977;10:332–9.
- [21] McLeish TCB, Milner ST. *Adv Polym Sci* 1999;143:195–256.
- [22] Vega JF, Santamaria A, Munoz-Escalona A, Lafuente P. *Macromolecules* 1998;31:3639–47.

- [23] Malmberg A, Liimatta J, Lehtinen A, Lofgren B. *Macromolecules* 1999;32:6687–96.
- [24] Wood-Adams PM, Dealy JM, deGroot AW, Redwine OD. *Macromolecules* 2000;33:7489–99.
- [25] Lohse DJ, Milner ST, Fetters LJ, Xenidou M, Hadjichristidis N, Mendelson RA, Garcia-Franco CA, Lyon MK. *Macromolecules* 2002;35:3066–75.
- [26] Gabriel C, Munstedt H. *Rheol Acta* 2002;41:232–42.
- [27] Kim EK, Bae JS, Im SS, Kim BC, Han YK. *J Appl Polym Sci* 2001;80:1388–94.
- [28] Chae HG, Kim BC, Im SS, Han YK. *Polym Engng Sci* 2001;41:1133–9.
- [29] Priddy DB, Kohler B, Kumpf RJ, Pielartzik H. US Patent 5,693,722; 1997.
- [30] Bolton DH, Wooley KL. *Macromolecules* 1997;30:1890–6.
- [31] Wimberger-Friedl R, Hut MGT, Schoo HFM. *Macromolecules* 1996;29:5453–8.
- [32] Wool RP. *Macromolecules* 1993;26:1564–9.
- [33] Gabriel C, Kaschta J. *Rheol Acta* 1998;37:358–64.
- [34] Cox WP, Merz EH. *J Polym Sci* 1958;28:619–22.
- [35] Graessley WW. *Adv Polym Sci* 1974;16:1–284.
- [36] Dealy JM, Wissbrum KF. *Melt rheology and its role in plastics processing: theory and applications*. New York: Van Nostrand Reinhold; 1990. Chapter 10.
- [37] de Gennes PG. *J Phys* 1975;36:1199–203.
- [38] Kasehagen LJ, Macosko CW, Trowbridge D, Magnus F. *J Rheol* 1996;40:689–709.
- [39] Milner ST, McLeish TCB, Young RN, Hakiki A, Johnson JM. *Macromolecules* 1998;31:9345–53.
- [40] Han CD, John MS. *J Appl Polym Sci* 1986;32:3809–40.
- [41] Han CD, Kim JK. *Polymer* 1993;34:2533–9.
- [42] Han CD, Baik DM, Kim JG. *Macromolecules* 1990;23:561–70.
- [43] Wang J, Porter RS. *Rheol Acta* 1995;34:496–503.
- [44] Graessley WW. *Macromolecules* 1982;15:1164–7.
- [45] Rochefort WE, Smith GG, Rachapudy H, Raju VR, Graessley WW. *J Polym Sci, Phys Ed* 1979;17:1197–210.
- [46] Masuda T, Ohta Y, Onogi S. *Macromolecules* 1971;4:763–8.
- [47] Gabriel C, Munstedt H. *Rheol Acta* 1999;38:393–403.
- [48] Graessley WW. *J Polym Sci, Phys Ed* 1980;18:27–34.
- [49] Doi M, Edwards SF. *J Chem Soc, Faraday Trans* 1978;74:1789–801.
- [50] Steeman PAM, Turnhout JV. *Macromolecules* 1994;27:5421–7.
- [51] Alegria A, Guerrica-Echevarria E, Goitiandia L, Telleria I, Colmenera J. *Macromolecules* 1995;28:1516–27.
- [52] Mertens IJA, Wubbenhorst M, Oosterbaan WD, Jenneskens LM, van Turnhout J. *Macromolecules* 1999;32:3314–24.
- [53] Nielsen LE. *Mechanical properties of polymers and composites*. New York: Marcel Dekker; 1974. Chapter 1.
- [54] Bohmer R, Ngai KL, Angell CA, Plazek DJ. *J Chem Phys* 1993;99:4201–6.
- [55] Hodge IM. *J Res Natl Inst Stand Technol* 1997;102:195–205.
- [56] Zhong ZZ, Schuele DE, Smith SW, Gordon WL. *Macromolecules* 1993;26:6403–9.
- [57] Pratt GJ, Smith MJA. *Polym Int* 1996;40:239–49.
- [58] Davidson DW, Cole RH. *J Chem Phys* 1950;18:1417.
- [59] McCrum NG, Read BE, Williams G. *Anelastic and dielectric effects in polymeric solids*. London: Wiley; 1967. Chapter 4.